

A model for mixed warm and hot right-handed neutrino dark matter

Maíra Dutra^a , Vinícius Oliveira^b , C. A de S. Pires^b , Farinaldo S. Queiroz^{c,d}

^a*Ottawa-Carleton Institute for Physics, Carleton University, 1125 Colonel By Drive, Ottawa, Ontario K1S 5B6, Canada*

^b*Departamento de Física, Universidade Federal da Paraíba, Caixa Postal 5008, 58051-970, João Pessoa, PB, Brazil*

^c*International Institute of Physics, Universidade Federal do Rio Grande do Norte, Campus Universitário, Lagoa Nova, Natal-RN 59078-970, Brazil*

^d*Departamento de Física, Universidade Federal do Rio Grande do Norte, 59078-970, Natal, RN, Brasil*

E-mail: mdutra@physics.carleton.ca, vlbo@academico.ufpb.br,
cpires@fisica.ufpb.br, farinaldo.queiroz@iip.ufrn.br

ABSTRACT: We discuss a model where a mixed warm and hot keV neutrino dark matter rises naturally. We arrange active and sterile neutrinos in the same $SU(3)_L$ multiplet, with the lightest sterile neutrino being dark matter. The other two heavy sterile neutrinos, through their out-of-equilibrium decay, contribute both to the dilution of dark matter density and its population, after freeze-out. We show that this model features all ingredients to overcome the overproduction of keV neutrino dark matter, and explore the phenomenological implications for Big Bang Nucleosynthesis and the number of relativistic degrees of freedom.

Contents

1	Introduction	1
2	The essence of the $331\nu_R$ model	3
2.1	Particle content	3
2.2	Neutrino Masses	4
2.3	Main interactions	5
3	Relic abundance of a light sterile neutrino	6
3.1	Relativistic freeze-out	8
3.2	Non-thermal production	9
4	Coupled evolution of sterile neutrinos	10
4.1	Numerical results	12
5	Viable parameter space	14
5.1	Contribution to ΔN_{eff}	15
5.2	Structure formation (free-streaming)	15
6	Conclusions	17
A	N_1 temperature at the matter-radiation equality	18
B	Evaluation of ΔN_{eff}	19

1 Introduction

Although there is no doubt about the existence of dark matter (DM)[1, 2], we have no idea about its nature. There are compelling pieces of evidence that dark matter may be composed of elementary particles, all based on its gravitational interaction with ordinary matter. Such particles must be electrically neutral (at least effectively) and cosmologically stable. Dark matter is also crucial for evolution of structure formation as we observe today. In general, dark matter candidates are classified as hot dark matter (HDM), warm dark matter (WDM), or cold dark matter (CDM) depending on their free-streaming around the period of structure formation. Structure formation requirements do not allow for dark matter to be comprised of mostly HDM [3].

Weakly interacting massive particles (WIMPs) are by far the most extensively studied class of CDM as the correct dark matter abundance is easily reproduced with cross sections

around the weak scale [4]. They have been extensively searched for by many experiments (direct and indirect detection, and colliders) with no success [5]. The null results reported thus far motivate us to explore alternative candidates. As CDM faces problems at small-scale astrophysical scales, mixed populations of dark matter are well motivated [6]. Right-handed neutrinos (from now on sterile neutrinos) with mass around keV scale are suitable candidates. Sterile neutrinos arise in many popular extensions of the standard model (SM) such as left-right model [7–9], B-L model [10–13] and in the 3-3-1 model with right-handed neutrinos ($331\nu_R$) [14–16].

Although interesting alternatives to CDM candidates, keV sterile neutrinos are usually overproduced in simplified models [17]. In this case, the most plausible way to *dilute* this dark matter population and obtain the correct abundance is through entropy injection [18]. In general, entropy can be injected into the early universe when a long-lived particle, a *diluton*, that decouples while relativistic, dominates the energy density of the universe and decays once non-relativistic [18]. Thus, a successful keV dark matter model should feature a long-lived particle that plays the role of such diluton. The natural diluton candidates are the right-handed neutrino themselves. The lightest right-handed neutrino is stable, while the other two act as the diluton [19–21]. This apparent easy solution faces solid constraints from Big Bang Nucleosynthesis (BBN) and the Cosmic Microwave Background (CMB).

The study of keV neutrino dark matter has been discussed elsewhere in simplified models, our goal here is to embed this mechanism in a UV complete model, which is well motivated for other theoretical reasons. We will discuss this keV neutrino dark matter in a model based on the $SU(3)_C \times SU(3)_L \times U(1)_N$ gauge symmetry, 331 for short. There are several ways to arrange the fermion generations in this gauge symmetry. The different ways give rise to different models. Here we will focus on the $331\nu_R$ [14–16], which features right-handed neutrinos in the same $SU(3)_L$ multiplet of the active neutrinos [22].

In this work, we check under which conditions the $331\nu_R$ accommodates a successful keV dark matter candidate. To do so, we invoke a discrete symmetry to guarantee the stability of the lightest sterile neutrino. We calculate the relativistic freeze-out of the lightest sterile neutrino and consider the heavier ones as dilutons. As we are dealing with an extended gauge sector there are new interactions that impact the sterile neutrino abundance, differing from past keV neutrino dark matter studies. We highlight that the two heavy sterile neutrinos dilute and produce dark matter. To test our model, we estimate the free-streaming length of our dark matter candidate and find that we have a mixed WDM+HDM scenario, which successfully obeys the constraints stemming from CMB and BBN.

This work is organized as follows. In [Section 2](#) we present the key aspects of the model; in [Section 3](#) and [Section 4](#) we address the production mechanisms; in [Section 5](#) we outline the viable parameter space; lastly in we draw our conclusions in [Section 6](#).

2 The essence of the $331\nu_R$ model

2.1 Particle content

In the $331\nu_R$ model the lepton generations are arranged as,

$$L_l = \begin{pmatrix} \nu_{lL} \\ e_{lL} \\ (\nu_{lR})^c \end{pmatrix} \sim (1, 3, -1/3), \quad e_{lR} \sim (1, 1, -1), \quad (2.1)$$

where $l = e, \mu, \tau$ refers to the three generations.

In the quark sector, anomaly cancellation requires the first two generations of quarks to come in the triplet representation, while the third in anti-triplet representation as,

$$\begin{aligned} Q_{iL} &= \begin{pmatrix} d_i \\ -u_i \\ d'_i \end{pmatrix}_L \sim (3, \bar{3}, 0), \quad u_{iR} \sim (3, 1, 2/3), \\ d_{iR} &\sim (3, 1, -1/3), \quad d'_{iR} \sim (3, 1, -1/3), \\ Q_{3L} &= \begin{pmatrix} u_3 \\ d_3 \\ u'_3 \end{pmatrix}_L \sim (3, 3, 1/3), \quad u_{3R} \sim (3, 1, 2/3), \\ d_{3R} &\sim (3, 1, -1/3), \quad u'_{3R} \sim (3, 1, 2/3) \end{aligned} \quad (2.2)$$

where $i = 1, 2$. The new quarks (u' , d') have the usual electric charges.

The gauge sector of the model is formed by the standard gauge bosons, A , W^\pm and Z , and five others called W'^\pm , U^0 , $U^{0\dagger}$ and Z' . The interactions of these gauge bosons with matter can be found in Ref. [23].

The scalar sector of the original version involves three scalar triplets, namely $\eta = (\eta^0, \eta^-, \eta^{0'})^T \sim (\mathbf{1}, \mathbf{3}, -1/3)$, $\chi = (\chi^0, \chi^-, \chi^{0'})^T \sim (\mathbf{1}, \mathbf{3}, -1/3)$, and $\rho = (\rho^+, \rho^0, \rho^{+'})^T \sim (\mathbf{1}, \mathbf{3}, 2/3)$. The quantum numbers under $SU(3)_C \times SU(3)_L \times U(1)_N$ are displayed in parenthesis

With such scalar content, when the symmetry $SU(3)_C \times SU(3)_L \times U(1)_N$ is spontaneously broken to $SU(3)_C \times U(1)_{em}$, all particles acquire masses at tree level, except the neutrinos.

We adopt the following vacuum structure,

$$\langle \eta \rangle_0 = \begin{pmatrix} \frac{v_\eta}{\sqrt{2}} \\ 0 \\ 0 \end{pmatrix}, \quad \langle \rho \rangle_0 = \begin{pmatrix} 0 \\ \frac{v_\rho}{\sqrt{2}} \\ 0 \end{pmatrix}, \quad \langle \chi \rangle_0 = \begin{pmatrix} 0 \\ 0 \\ \frac{v_{\chi'}}{\sqrt{2}} \end{pmatrix}, \quad (2.3)$$

which implies that $v_\eta^2 + v_\rho^2 = (246)^2 \text{GeV}^2$, to make sure that $M_W^2 = g^2(v_\eta^2 + v_\rho^2)/4$ in agreement with the Standard Model.

To further simplify the model, we assume the following discrete symmetry transformation over the full Lagrangian,

$$(\eta, \rho, e_{lR}, u_{aR}, d_{aR}) \rightarrow -(\eta, \rho, e_{lR}, u_{aR}, d_{aR}), \quad (2.4)$$

where $a = 1, 2, 3$. This discrete symmetry (Z_2) will play an important role in the dark sector of the model, as we shall see. With such matter and scalar content we build the following Yukawa interactions invariant under the gauge symmetry,

$$\begin{aligned}\mathcal{L}^Y = & \lambda_{ij}^1 \bar{Q}_{iL} \chi^* d'_{jR} + \lambda_{33}^2 \bar{Q}_{3L} \chi u'_{3R} + \lambda_{ia}^3 \bar{Q}_{iL} \eta^* d_{aR} + \\ & \lambda_{3a}^4 \bar{Q}_{3L} \eta u_{aR} + \lambda_{ia}^5 \bar{Q}_{iL} \rho^* u_{aR} + \lambda_{3a}^6 \bar{Q}_{3L} \rho d_{aR} + \\ & G_{ll'} \bar{L}_{lL} \rho e_{l'_R} + \text{H.c.}\end{aligned}\quad (2.5)$$

which generate masses for all fermions, with the exception of neutrinos.

We remark that while the SM does not contain any dark matter candidate, the $331\nu_R$ model poses three candidates, namely, η^0 , U^0 or ν_R , which are mutually exclusive. U^0 is underabundant, while η^0 and ν_R are viable multi-TeV dark matter candidates [24–33]. Concerning U^0 , despite of being an interesting candidate, unfortunately it does not provide the correct abundance (it is under-abundant), while ν_R did not receive any attention until now. In other words, this is the first time that right-handed neutrino is being treated as dark matter in the $331\nu_R$.

Before considering ν_R as dark matter candidate we discuss in the next section how to generate masses for the neutrinos in the model.

2.2 Neutrino Masses

Right-handed neutrinos are hypothetical particles and their masses are free parameters that may be in a wide range of values varying from eV up to GUT scale. In the original version of the $331\nu_R$ model neither ν_L nor ν_R gain masses. In view of this the most immediate way of providing masses for them is through effective dimension-5 operators[22]. In the case of left-handed neutrinos, this operator is constructed with the scalar triplet η and the lepton triplet L ,

$$\mathcal{L}_{\nu_L} = \frac{f_{ll'}}{\Lambda} \left(\overline{L}_l^C \eta^* \right) \left(\eta^\dagger L_{l'} \right) + \text{H.c.} \quad (2.6)$$

According to this operator, when η^0 develops a VEV, v_η , the left-handed neutrinos develop Majorana mass terms,

$$(m_{\nu_L})_{ll'} = \frac{f_{ll'} v_\eta^2}{\Lambda}. \quad (2.7)$$

Regarding right-handed neutrinos, the dimension-5 operator that give them mass is constructed with the scalar triplet χ and the lepton triplet L ,

$$\mathcal{L}_{\nu_R} = \frac{h_{ll'}}{\Lambda} \left(\overline{L}_l^C \chi^* \right) \left(\chi^\dagger L_{l'} \right) + \text{H.c.} \quad (2.8)$$

When χ'^0 develops a VEV, $v_{\chi'}$, this effective operator provides Majorana masses for the right-handed neutrinos,

$$(m_{\nu_R})_{ll'} = \frac{h_{ll'} v_{\chi'}^2}{\Lambda}. \quad (2.9)$$

Once $v_{\chi'} > v_\eta$, then $m_{\nu_R} > m_{\nu_L}$. Thus, light right-handed neutrinos is a natural result of the model.

Observe that the discrete symmetry discussed above avoids the operator $\sim \frac{1}{\Lambda}(L\eta)(\chi L)$ which would generate mixing among active and sterile neutrinos. This is a particularly interesting result, as it renders the lightest right-handed neutrino automatically stable and suitable to be our dark matter candidate. For the realization of these effective operators, see Refs. [34–36].

2.3 Main interactions

To work with the physical neutrinos we have to diagonalize m_{ν_L} and m_{ν_R} . From now on we refer to the active physical neutrinos as $\nu_L = (\nu_1, \nu_2, \nu_3)_L^T$, and to the physical sterile ones as $N_L = (N_1^C, N_2^C, N_3^C)_L^T$. To simplify even more we assume ν_R in a diagonal basis.

We now present the interactions involving sterile neutrinos that matter for us here:

$$\mathcal{L}_{W'} = -\frac{g}{\sqrt{2}} \bar{N}_L \gamma^\mu l_L W_\mu'^+ + \text{H.c.} \quad (2.10)$$

$$\mathcal{L}_{U^0} = -\frac{g}{\sqrt{2}} \bar{\nu}_L (U_{PMNS}^T) \gamma^\mu N_L U_\mu^0 + \text{H.c.} \quad (2.11)$$

$$\begin{aligned} \mathcal{L}_{Z'} = & -\frac{g}{2C_W} \left(\frac{(1-2S_W^2)}{\sqrt{3-4S_W^2}} [\bar{\nu}_L \gamma^\mu \nu_L] - \frac{2C_W^2}{\sqrt{3-4S_W^2}} [\bar{N}_L \gamma^\mu N_L] \right) Z_\mu' \\ & - \frac{g}{4C_W \sqrt{3-4S_W^2}} \bar{l} \gamma^\mu ((3-4C_W^2) + \gamma_5) l Z_\mu', \end{aligned} \quad (2.12)$$

where $C_W = \cos(\theta_W)$ and $S_W = \sin(\theta_W)$ with θ_W being the Weinberg angle and $l = (e, \mu, \tau)^T$.

The dominant interactions involving quarks that matter for the calculation of the dark matter abundance are

$$\begin{aligned} \mathcal{L}_{Z'} = & -\frac{g}{2C_W} \frac{\sqrt{3-4S_W^2}}{3} [\bar{u}_L \gamma^\mu u_L] Z_\mu' - \frac{g}{2C_W} \frac{2(1-S_W^2)}{\sqrt{3-4S_W^2}} [\bar{t}_L \gamma^\mu t_L] Z_\mu' \\ & - \frac{g}{2C_W} \frac{\sqrt{3-4S_W^2}}{3} [\bar{d}_L \gamma^\mu d_L] Z_\mu' - \frac{g}{2C_W} \frac{2(1-S_W^2)}{\sqrt{3-4S_W^2}} [\bar{b}_L \gamma^\mu b_L] Z_\mu', \end{aligned} \quad (2.13)$$

where $u = (u, c)^T$ and $d = (d, s)^T$.

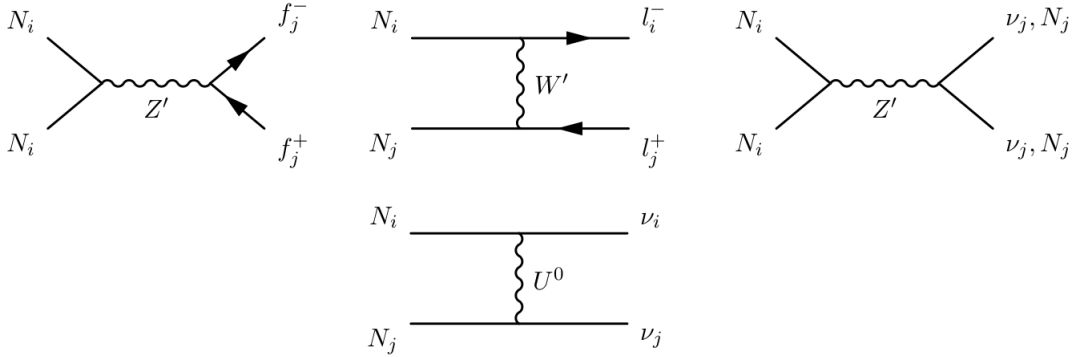


Figure 1: Processes that contribute to N_i freeze-out where f represents the charged fermions of standard models and l represents the charged leptons with $i, j = 1, 2, 3$.

3 Relic abundance of a light sterile neutrino

We assume that N_1 is the lightest of the sterile neutrinos, being in principle a dark matter candidate. We therefore check under which conditions it thermalizes with species of the standard model bath in the early universe and calculate its relic abundance accordingly.

In the context of the $331\nu_R$ model, the sterile neutrinos are able to thermalize with the standard fermions through exchanges of W' , Z' and U^0 , as depicted in Fig. 1. This happens whenever their interaction rates $\Gamma_{N_i}(T)$ are faster than the Hubble rate $H(T)$ at a given temperature T :

$$\frac{\Gamma_{N_i}(T)}{H(T)} \gg 1. \quad (3.1)$$

The rate at which N_i self-annihilate into species 3 and 4, with masses m_{N_3} and m_{N_4} , is given by $\Gamma_{N_i}(T) = n_{N_i}^{eq}(T)\langle\sigma v\rangle$, with $n_{N_i}^{eq}(T)$ their equilibrium number density and a thermally averaged annihilation cross-section given by

$$\langle\sigma v\rangle \equiv \frac{1}{(n_{N_i}^{eq}(T))^2} \frac{\mathcal{S}}{32(2\pi)^6} T \int ds \frac{\sqrt{\lambda(s, m_{N_1}^2, m_{N_1}^2)}}{s} \frac{\sqrt{\lambda(s, m_{N_3}^2, m_{N_4}^2)}}{\sqrt{s}} K_1\left(\frac{\sqrt{s}}{T}\right) \int d\Omega |\mathcal{M}|^2, \quad (3.2)$$

where \mathcal{S} is the symmetrization factor, s is the Mandelstam variable, $\lambda(x, y, z)$ is the Källen function, K_i is the modified Bessel function of the second kind of order i , Ω is the solid angle between initial and final states in the center of mass frame, and $|\mathcal{M}|^2$ the (not averaged) squared amplitude of the process.

As usual, we compute the freeze-out temperatures T_f at which the sterile neutrinos decouple from the thermal bath by equaling $n_{N_i}^{eq}(T_f)\langle\sigma v\rangle(T_f) = H(T_f)$ for the main processes. For simplicity but without loss of generality for our purposes, we will assume the hierarchy $m_{N_3} \gg m_{N_2} \gg m_{N_1}$. As a consequence, we can neglect co-annihilation processes [37].

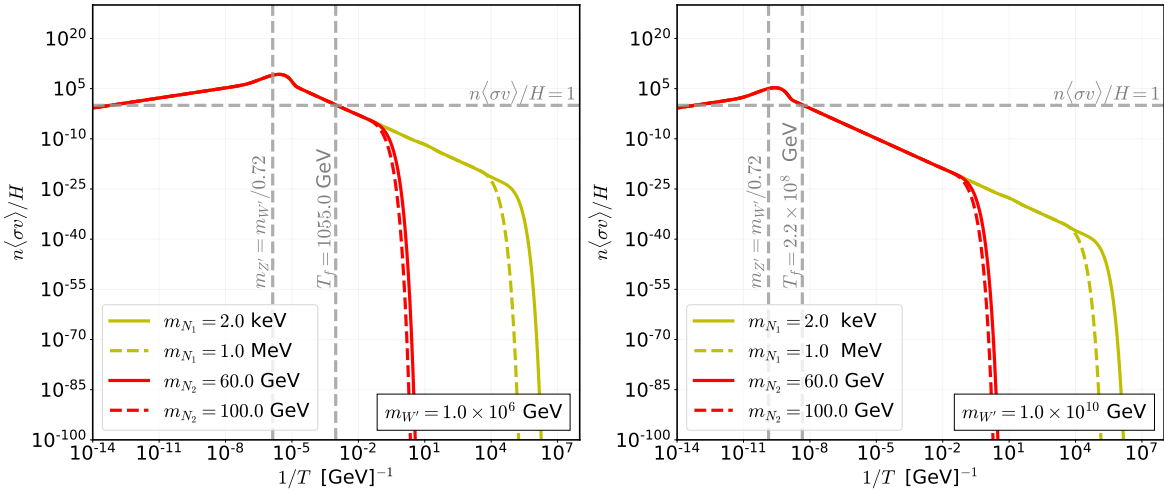


Figure 2: Ratio between the interaction rates $\Gamma \equiv n\langle\sigma v\rangle$ and the Hubble rate H for N_1 (yellow) and N_2 (red) annihilations as a function of the inverse of temperature. The left panel accounts for $m_{W'} = 1.0 \times 10^6$ GeV and the right panel, for $m_{W'} = 1.0 \times 10^{10}$ GeV. The dashed horizontal line represents $\Gamma/H = 1$, below which the sterile neutrinos are decoupled. The dashed vertical lines indicates where $T = m_{Z'}$ and $T = T_f$.

In Fig. 2 we show the ratio between the annihilation rates of N_1 (in yellow) and of N_2 (in red) and the Hubble rate in the standard case of a radiation-dominated era as a function of the inverse of temperature¹ for $m_{W'} = 1.0 \times 10^6$ GeV (left panel) and $m_{W'} = 1.0 \times 10^{10}$ GeV (right panel). To obtain the curves of Fig. 2 we consider all annihilation processes shown in Fig. 1. This analysis is also applicable to the case of N_3 , but for the purpose of this paper we do not need to take it into account, as we will see later. As shown in Fig. 2, the freeze-out temperature T_f increases with the mass of the mediator. In our model, the gauge bosons have similar masses, and from now on we assume $m_{W'} = m_{U^0} \simeq 0.72 \times m_{Z'}$ [23]. We can see in Fig. 2 that the maximum of the ratio happens when the gauge bosons are produced on-shell, making the decoupling to take place close to that scale.

We have chosen in Fig. 2 masses of N_1 , N_2 , and W' close to the values which will provide the right amount of relic abundance for N_1 , as we will show later. In such a case, we can see that N_1 and N_2 freeze-out almost at the same time (when $n_{N_i}\langle\sigma v\rangle \sim H$, as indicated by the dashed horizontal line), with $T_f \simeq 1.0 \times 10^3$ GeV for $m_{W'} = 1.0 \times 10^6$ GeV (left panel) and $T_f \simeq 2.2 \times 10^8$ GeV for $m_{W'} = 1.0 \times 10^{10}$ GeV (right panel). Thus, both N_1 and N_2 decouple while still relativistic. As shown in Fig. 2 the freeze-out temperature T_f strongly depends of mediator mass, for that benchmark value of mass. When the masses of N_1 and N_2 increase (indicated by the yellow and red dashed curves in Fig. 2, respectively) the Boltzmann suppression (which occur when $m_{N_i} \sim T$) occurs earlier, as shown in Fig. 2. Given that in our model the couplings between sterile neutrinos, gauge bosons, and standard fields are all

¹For our numerical results, we have used the CUBA library [38].

of order $\mathcal{O}(10^{-1})$, the only way of avoiding thermalization of sterile neutrinos is by invoking gauge bosons heavier than about $\mathcal{O}(10^{16})$ GeV.

We remark that among all processes contributing to the freeze-out of N_1 and N_2 , the most relevant are annihilations into SM charged leptons and active neutrinos. In the relevant limit of $m_{N_i} \ll T \ll m_{W'}$, they happen at the following rate:

$$n_{N_i} \langle \sigma v \rangle \simeq \frac{16}{9} \frac{T^5 G_F^2}{\zeta(3) (2\pi)^4} \left(\frac{m_W}{m_{W'}} \right)^4 \left(64 - 8 \left(\frac{m_{W'}}{m_{Z'}} \right)^2 \right). \quad (3.3)$$

We have found the typical freeze-out temperature to be given by

$$T_f \simeq 1.7 \left(\frac{m_{W'}}{m_W} \right)^{4/3} g_e^{1/6} (T_f) \text{ MeV}, \quad (3.4)$$

where $g_e(T_f)$ is the number of energetic degrees of freedom at freeze-out, with $g_e(T_f) \sim 100$ for $T_f > 100$ GeV. We have checked that our numerical solution shown in Fig. 2 is in a good agreement with the estimation above.

We can therefore conclude that N_1 would be a cosmic relic which was once thermalized, and proceed with the computation of their final abundance in order to determine whether it can constitute the cosmological dark matter.

3.1 Relativistic freeze-out

The final relic abundance of N_1 is defined to be

$$\frac{\Omega_{N_1}^0 h^2}{0.12} \simeq \frac{m_{N_1}}{1 \text{ GeV}} \frac{Y_{N_1}^0}{4.34 \times 10^{-10}}, \quad (3.5)$$

where the label "⁰" indicates quantities as measured today, with $\Omega_{DM}^0 h^2 \simeq 0.12$ being inferred by the Planck satellite [2], and $Y_i \equiv n_i/s$ is the yield of a species i , with s the entropy density in a comoving volume.

In this work, we are interested in the case of a light sterile neutrino dark matter. For N_1 thermally produced the lower limit on its mass is $m_{N_1} \gtrsim 2.0$ keV [39]. As we have just seen, for the mass hierarchy $m_{N_1}, m_{N_2} \ll m_{W'}$, both N_1 and N_2 decouple from the thermal bath almost simultaneously and at high temperatures ($T \sim m_{W'}/100$). The yield of a Majorana neutrino that decouples while ultra-relativistic is given by

$$Y_{N_i}(T) = \frac{135\zeta(3)}{4\pi^4 g_s(T_f)}, \quad (3.6)$$

for temperatures T below their freeze-out temperature T_f , where $g_s(T_f)$ is the number of entropic degrees of freedom at freeze-out.

Therefore, if $Y_{N_1}^0 = Y_{N_1}(T_f)$, the agreement with the relic abundance constraint,

$$\frac{\Omega_{N_1}^0 h^2}{0.12} \simeq \left(\frac{m_{N_1}}{1 \text{ keV}} \right) \left(\frac{1000}{g_s(T_f)} \right), \quad (3.7)$$

would require an unreasonable amount of relativistic degrees of freedom by the time of freeze-out in order for a light sterile neutrino to not overclose the universe.

To the best of our knowledge, the only way of depleting the yield of a decoupled species is by considering entropy production after freeze-out. As it is well known [40], a long-lived particle that decoupled while ultra-relativistic can dominate the cosmic expansion before decaying, thus injecting a sizable amount of entropy into the thermal bath. It is therefore interesting to notice that the heavier sterile neutrinos are natural candidates to deplete the yield of N_1 . For simplicity, we will investigate the out-of-equilibrium decay of N_2 as the source of entropy production, while assuming that N_3 is heavy enough as to not affect our analysis.

It is straightforward to see that an increase of total entropy S in a comoving volume after the freeze-out of any relic, by a factor of $\Delta \sim S(T_0)/S(T_f)$, will dilute its yield by the same factor: $Y_{N_i}(T_0) = Y_{N_i}(T_f)/\Delta$. For freeze-out happening at TeV scale, our model provides $g_s(T_f) \sim 100$. Thus, N_1 with mass in the keV-MeV range requires an entropy injection of $\Delta = 10 - 100$ in order to be a viable dark matter candidate. As we show in what follows, though, the out-of-equilibrium decay of N_2 contributes in a non-trivial way to the final abundance of N_1 in the context of the $331\nu_R$ model.

3.2 Non-thermal production

As we have just discussed, the out-of-equilibrium decay of N_2 into species of the thermal bath dilutes the abundance of our dark matter candidate, N_1 . However, in the $331\nu_R$ model, tree-body decays of N_2 into N_1 can be sizable, which could potentially repopulate (and overclose) the universe with dark matter. Therefore, the final relic abundance of N_1 will have a (thermal) contribution from the relativistic freeze-out and also a (non-thermal) contribution from the tree-body decays of N_2 into N_1 :

$$\Omega_{N_1}^0 h^2 = \Omega_{N_1}^0 h^2 \Big|_{\text{thermal}} + \Omega_{N_1}^0 h^2 \Big|_{\text{non-thermal}}. \quad (3.8)$$

Let us parametrize the total decay width of N_2 in terms of the partial width into N_1 , $\Gamma_{N_2}^{(N_1)}$:

$$\Gamma_{N_2} \equiv (1 + \alpha) \Gamma_{N_2}^{(N_1)}. \quad (3.9)$$

The dimensionless parameter $\alpha = \sum_i \Gamma_{N_2}^i / \Gamma_{N_2}^{(N_1)}$ contains all other channels which do not involve N_1 as final product ². Of course, N_2 must decay into species which thermalize with the SM bath in order to dilute N_1 . Decay channels into $331\nu_R$ states do not necessarily thermalize, but here we will treat α as a free parameter encoding only decay channels which instantaneously thermalize with the SM bath.

We have found that the leading contributions to $\Gamma_{N_2}^{(N_1)}$ are the three-body decays into charged leptons and neutrinos. In the limit $m_{N_1}, m_l \ll m_{N_2} \ll m_{W'}$, we have

$$\Gamma_{N_2}^{(N_1)} \equiv \Gamma_{N_2 \rightarrow \mu e N_1} + \Gamma_{N_2 \rightarrow \nu_\mu \nu_e N_1} \approx \frac{G_F^2}{96\pi^3} m_{N_2}^5 \left(\frac{m_W^4}{m_{W'}^4} + \frac{m_W^4}{m_U^4} \right). \quad (3.10)$$

²All those processes are mediated by the scalars of the model and involve only standard fermions as final product as for example $N_2 \rightarrow l^\pm + \text{hadrons}$.

In the next section, we develop the tools needed to properly dealing with the competing effects of the N_2 out-of-equilibrium decays.

4 Coupled evolution of sterile neutrinos

Let us now discuss how to properly find the final relic abundance of our dark matter candidate, the keV scale sterile neutrino N_1 . The relativistic freeze-out of both N_1 and N_2 , as well as the non-thermal production and dilution of N_1 due to the out-of-equilibrium decay of N_2 , can be taken into account by solving the following coupled Boltzmann fluid equations for the yields of N_1 and N_2 ³:

$$\begin{aligned}\frac{dY_{N_1}}{da} &= \frac{R_{N_1}(a, Y_{N_1}, Y_{N_2})}{s H(a) a} - \frac{Y_{N_1}}{S} \frac{dS}{da} \\ \frac{dY_{N_2}}{da} &= \frac{R_{N_2}(a, Y_{N_1}, Y_{N_2})}{s H(a) a} - \frac{Y_{N_2}}{S} \frac{dS}{da},\end{aligned}\quad (4.1)$$

where the scale factor a is used as a time parameter.

The relativistic freeze-out and the non-thermal production of N_1 are accounted for by the first term in the right hand side of the equation above, whereas the second term accounts for the dilution of Y_{N_1} after the entropy production.

The reaction rate densities R_{N_1, N_2} contain all processes that can change the number of N_1 and N_2 in a comoving volume. We have found the following leading contributions:

$$\begin{aligned}R_{N_1} &\approx -s^2 \langle \sigma v \rangle_{N_1 N_1} \left(Y_{N_1}^2 - \left(Y_{N_1}^{(eq)} \right)^2 \right) + s \langle \Gamma_{N_2}^{(N_1)} \rangle \left(Y_{N_2} - Y_{N_1} \frac{Y_{N_2}^{(eq)}}{Y_{N_1}^{(eq)}} \right) \\ R_{N_2} &\approx -s^2 \langle \sigma v \rangle_{N_2 N_2} \left(Y_{N_2}^2 - \left(Y_{N_2}^{(eq)} \right)^2 \right) - s \langle \Gamma_{N_2}^{(N_1)} \rangle \left(Y_{N_2} - Y_{N_1} \frac{Y_{N_2}^{(eq)}}{Y_{N_1}^{(eq)}} \right) \\ &\quad - \alpha s \langle \Gamma_{N_2}^{(N_1)} \rangle \left(Y_{N_2} - Y_{N_2}^{(eq)} \right).\end{aligned}\quad (4.2)$$

The terms proportional to $\langle \sigma v \rangle_{N_i N_i}$ represent the annihilations into SM leptons (see Eq. (3.3)) and their backreactions. We can represent $\langle \sigma v \rangle_{N_i N_i}$ as the sum of the channels that contribute for it:

$$\begin{aligned}\langle \sigma v \rangle_{N_i N_i} &= \langle \sigma v \rangle_{N_i N_i \rightarrow e \bar{e}} + \langle \sigma v \rangle_{N_i N_i \rightarrow \mu \bar{\mu}} + \langle \sigma v \rangle_{N_i N_i \rightarrow \tau \bar{\tau}} + \langle \sigma v \rangle_{N_i N_i \rightarrow \nu_e \bar{\nu}_e} + \\ &\quad \langle \sigma v \rangle_{N_i N_i \rightarrow \nu_\mu \bar{\nu}_\mu} + \langle \sigma v \rangle_{N_i N_i \rightarrow \nu_\tau \bar{\nu}_\tau}.\end{aligned}\quad (4.3)$$

The other terms represent the contribution of the N_2 decays and inverse decays. We recall that α encodes the channels without N_1 as a decay product, assuming that they all thermalize instantaneously. We therefore see that the decay of N_2 into N_1 couples their evolution in the early universe, even if the entropy production were negligible.

³We recall that we consider the hierarchy $m_{N_1} \ll m_{N_2} \ll m_{N_3}$, such that N_3 decays at much higher temperatures and does not significantly affect the lighter sterile neutrinos.

In order to inject a significant amount of entropy into the thermal bath after decaying, N_2 must be significantly long-lived and have dominated the total energy density of the universe. This is indeed a natural consequence of our framework, since N_2 decouples while ultra-relativistic – which means that $\rho_{N_2}/\rho_R \propto m_{N_2}a$ once it becomes non-relativistic, with ρ_R the energy density of radiation. The Hubble rate in Eq. (4.1) will be therefore given by

$$H(a) = \frac{\sqrt{\rho_R(a) + \rho_{N_2}(a)}}{\sqrt{3}M_{Pl}}, \quad (4.4)$$

where $M_{Pl} \simeq 2.4 \times 10^{18}$ GeV is the reduced Planck mass.

From the temperature at which N_2 starts dominating the energy density, T_i , until its complete decay, at the so-defined reheat temperature T_{RH} , the universe would have therefore undergone an early matter-dominated era. The duration of such an era is determined by the amount of entropy produced, $T_i/T_{RH} \propto \Delta$, and the reheat temperature is found to be given by [41]

$$T_{RH} = \left(\frac{5\pi^2}{72} g_e(T_{RH}) \right)^{-1/4} \sqrt{\Gamma_{N_2} M_{Pl}}. \quad (4.5)$$

In order to not jeopardize the BBN predictions [42], we must ensure $T_{RH} \gtrsim 4$ MeV. This guarantees that N_2 decays before the weak decoupling of active neutrinos and all the standard leptons thermalize.

The rate of injection of entropy due to the decay of N_2 is given by [40],

$$\frac{dS}{da} = f_T \frac{\Gamma_{N_2}}{H} \frac{\rho_{N_2} a(t)^2}{T}, \quad (4.6)$$

where f_T represents the fraction of the decay products of N_2 that thermalize in the plasma [43, 44]. The fraction f_{NT} of decay products that do not thermalize will populate the sea of decoupled relativistic species (contributing to $\Delta N_{eff} \neq 0$, see Section 5.1).

It is therefore convenient to rewrite the energy density of N_2 in terms of f_T and f_{NT} :

$$\rho_{N_2} = \overbrace{\left[f_T^l \cdot Br(N_2 \rightarrow \mu e N_1) + f_T^\nu \cdot Br(N_2 \rightarrow \nu_\mu \nu_e N_1) + Br(N_2 \rightarrow others) \right]}^{f_T} \cdot \rho_{N_2} + \overbrace{\left[f_{NT}^l \cdot Br(N_2 \rightarrow \mu e N_1) + f_{NT}^\nu \cdot Br(N_2 \rightarrow \nu_\mu \nu_e N_1) \right]}^{f_{NT}} \cdot \rho_{N_2}, \quad (4.7)$$

where $Br(N_2 \rightarrow others) = 1/(1 + 1/\alpha)$ (see Eq. (3.9)) is the branching ratio into all decay channels without N_1 in final states.

Since $T_{RH} < T_f$, the N_1 produced via decay will not be able to thermalize anymore. This is why such dark matter population is said to be non-thermal. On the other hand, above 4 MeV, all SM leptons are able to thermalize. It is then easy to see that $f_T^l = f_T^\nu = 2/3$, whereas

$f_{NT}^l = f_{NT}^\nu = 1/3$, so that

$$\begin{aligned} f_T &= \frac{\alpha + 2/3}{1 + \alpha} \\ f_{NT} &= \frac{1/3}{1 + \alpha}. \end{aligned} \tag{4.8}$$

Finally, since ρ_{N_2} and ρ_R evolve non-trivially during the evolution of N_1 and N_2 , the set of Eq. (4.1) must be solved together with the following Boltzmann fluid equations:

$$\begin{aligned} \frac{d\rho_{N_2}}{dt} + 3H\rho_{N_2} &= -\rho_{N_2}\Gamma_{N_2} \\ \frac{d\rho_R}{dt} + 4H\rho_R &= \rho_{N_2}\Gamma_{N_2}. \end{aligned} \tag{4.9}$$

4.1 Numerical results

We numerically solve the set of equations (4.1), (4.4), (4.6), and (4.9). For numerical convenience, we re-scale the scale factor by $A \equiv aT_{RH}$, the energy density of N_2 by $\Phi_{N_2} \equiv \rho_{N_2}a^4$, and the energy density of radiation by $\Phi_R \equiv \rho_R a^4$.

Regarding the initial conditions, at $A = A^I \ll 1$ (the actual value does not change results), the yields of N_1 and N_2 follow their equilibrium values. The freeze-out of the sterile neutrinos take place while they are still relativistic, during the radiation era. From A^I until the moment when N_2 becomes non-relativistic, at $A = A_{NR}$, there is no entropy production and we just need to solve the coupled set of Eq. (4.1) without the last terms. In this case the Hubble rate is the usual one, $H \propto T^2/M_{Pl}$.

For $A \geq A_{NR}$, we consider the full set of equations. We follow Ref. [41] and assume an inflationary model that yield an inflationary reheat temperature of $T_{RH}^{Inf} \simeq 7 \times 10^{15}$ GeV, which implies $S^I = S^{NR} \simeq 897$ and $\Phi_R^I = \Phi_R^{NR} \simeq 1790$. At A_{NR} , both Y_{N_1} and Y_{N_2} are given by Eq. (3.6). Since at this point N_2 is non-relativistic, we have

$$\Phi_{N_2}^{NR} = m_{N_2} Y_{N_2}(T_f) \frac{S^{NR} A^{NR}}{T_{RH}}. \tag{4.10}$$

In Fig. 3 we present the evolution of the set of equations (4.1), (4.6), and (4.9) for $\alpha = 0, 10$ and 100 (continuous, dashed and dotted curves, respectively). On the left panel of Fig. 3 we show the full solutions for Y_{N_1} (blue curve) and Y_{N_2} (red curve), as well as the solution for Y_{N_1} in the absence of non-thermal contribution, $Y_{N_1}^{Thermal}$ (yellow curve). On the right panel we show the solutions for entropy S (pink curve) and for the quantities $\rho_{N_2}a^4$ (red curve) and $\rho_R a^4$ (green curve) and we can observe that when N_2 becomes non-relativistic (at A_{NR} , as shown) the energy density of radiation is still greater than the energy density of N_2 . However the ratio between the energy density of non-relativistic N_2 and the energy density of radiation evolves like $\rho_{N_2}/\rho_R \propto a m_{N_2}$, then ρ_{N_2} can dominate the energy density of the universe if N_2 is sufficiently long lived, as shown in Fig. 3. The complete decay of N_2 correspond in Fig. 3 to the abrupt decrease of Y_{N_2} on the left panel (or $\rho_{N_2}a^4$ on the right panel).

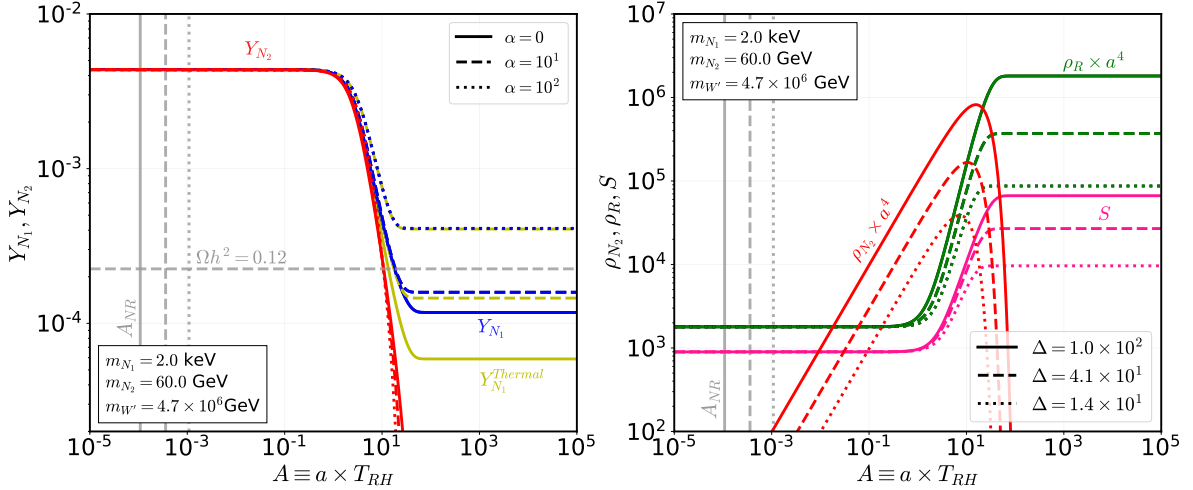


Figure 3: Evolution of coupled equations (4.1), (4.6), and (4.9) for $\alpha = 0, 10, 100$ (solid, dashed and dotted curves, respectively). Left panel: Evolution of total (thermal and non-thermal contribution) Y_{N_1} (blue), only thermal contribution $Y_{N_1}^{\text{Thermal}}$ (yellow) and Y_{N_2} (red). Right panel: Curves of entropy S (pink), $\rho_{N_2} \times a^4$ (red) and $\rho_R \times a^4$ (green), also shown are how the value of Δ changes as we increase α ($\Delta = 100, 41$ and 14 , for respective α).

We can observe in the right panel of Fig. 3 that when N_2 decays completely, the entropy is increased by a factor Δ and, as expected, it keeps constant before and after the decaying of N_2 . The increase of entropy dilutes the abundance of N_1 , as we have discussed, and we can observe this behavior from the evolution of the Y_{N_1} (blue curves) on the left panel in the Fig. 3. When N_2 decays completely, the injection of entropy ceases and Y_{N_1} , S and $\rho_R a^4$ levels off.

As shown in Fig. 3 the free parameter α plays an important role in the dilution of N_1 . Naively, one would expect that the dilution would increase with α , since more thermalized decay channels are allowed. However, since Γ_{N_2} increases with α , increasing α makes N_2 to decay earlier, such that it does not dominate the evolution of the universe long enough for a significant entropy injection to take place. We can observe this behavior on the right panel of Fig. 3: when $\alpha = 0$ (solid curves), $\rho_{N_2} > \rho_R$ for a much longer period and inject more entropy ($\Delta = 100$) than when we take $\alpha = 10^2$ (dotted curves) and obtain $\Delta = 14$. As the injection of entropy (parameterized by Δ) is responsible for diluting N_1 , this explains why the final value of Y_{N_1} is higher as we increase α .

The free parameter α has also an important role on the non-thermal contribution to the abundance of N_1 . As shown in the left panel of Fig. 3 there is a gap between Y_{N_1} (thermal and non-thermal contribution) and $Y_{N_1}^{\text{Thermal}}$ (only thermal contribution) which means that the N_1 produced via N_2 decays is responsible for increasing the abundance of N_1 from $Y_{N_1}^{\text{Thermal}}$ to Y_{N_1} . We can observe that this gap decreases as we increase α . This behavior is explained by the fact that when α increases, it allows N_2 to decay in another particles beyond N_1 .

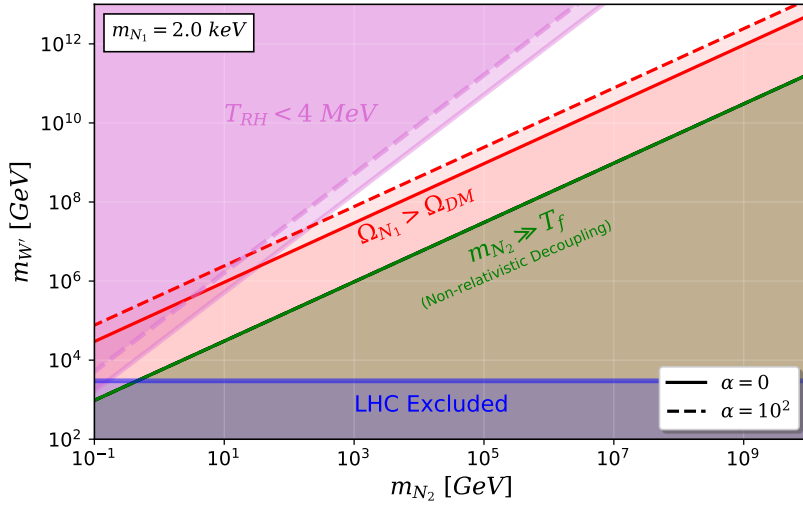


Figure 4: The continuous line represents the $\alpha = 0$ and the dashed-line represents $\alpha = 10^2$. The red line represents $\Omega_{N_1} h^2 = 0.12$. The constraint from BBN ($T_{RH} < 4 \text{ MeV}$) is in pink, LHC in blue ($m_{W'} < 3 \text{ GeV}$) and green shaded region represents the criteria to N_2 decouples ultra-relativistic.

According to our computation, for $\alpha = 10^2$ we have that the non-thermal contribution is approximately 1%, while for $\alpha = 0$ the non-thermal contribution is approximately 50%.

5 Viable parameter space

In this section we obtain the constraints on the parameter space $(m_{W'}, m_{N_2})$, that makes N_1 produced by means of relativistic freeze-out and diluted from N_2 decay a realistic DM candidate. In Fig. 4 we present these constraints for $\alpha = 0$ (solid curves) and $\alpha = 100$ (dashed curves).

Our first constraint is on the reheating temperature, given in Eq. (4.5), which is the temperature soon after the decay of N_2 . As we have pointed out, N_2 must decay prior to the active neutrinos decoupling as to not disturb the BBN predictions, such that we need to ensure $T_{RH} \gtrsim 4 \text{ MeV}$. In Fig. 4 the region in pink is excluded because it gives $T_{RH} < 4 \text{ MeV}$. As $T_{RH} \propto \sqrt{\Gamma_{N_2}}$ and Γ_{N_2} increases with α , this bound, translated to an upper limit on $M_{W'}$, is weakened as we increase α .

As we discussed above, N_2 must decouple ultra-relativistic in order to produce enough entropy and sufficiently dilute N_1 . This criterion rule out the green-shaded region in Fig. 4, in which $m_{N_1} \gg T_f$ with T_f given by Eq. (3.4). This bound is independent of the parameter α . Finally, the LHC constraint over the mediator mass, $m_{W'} \gtrsim 3 \text{ TeV}$ [45–48], is indicated by the blue-shaded region.

The correct relic abundance of N_1 today, $\Omega_{N_1}h^2 \simeq 0.12$, as constrained by the Planck satellite [2], is ensured by demanding

$$Y_{N_1}^0 \simeq 4.25 \times 10^{-4} \left(\frac{1 \text{ keV}}{m_{N_1}} \right). \quad (5.1)$$

In order to take into account the thermal and non-thermal contributions, we find $Y_{N_1}^0$ by solving Eq. (4.1) numerically. For this we developed a Python algorithm which searches the values of m_{N_2} and $m_{W'}$ obeying Eq. (5.1). The contours of correct relic density are shown by the solid and dashed red curves in Fig. 4, respectively for $\alpha = 0$ and $\alpha = 100$. The region below the red contours are excluded by Planck as they overclose the universe, while in the region above N_1 cannot account for all the dark matter but only for a fraction of it. As the purpose of this paper is to study N_1 as a viable DM candidate, we are interested in the red curves themselves.

5.1 Contribution to ΔN_{eff}

The amount of relativistic particles at matter-radiation equality epoch contributes to the number of relativistic degrees of freedom and directly affects the CMB power spectrum. An important parameter in this regard is the effective number of neutrino species defined as $N_{eff} = \frac{8}{7}(\frac{11}{4})^{4/3}(\frac{\rho_{rad} - \rho_\gamma}{\rho_\gamma})$, where ρ_{rad} and ρ_γ are respectively the total radiation and photon energy density. The current value for N_{eff} from Planck 2018+BAO [2] is $N_{eff} = 2.99 \pm 0.17$ which is in agreement with the standard model prediction $N_{eff}^{SM} = 3.046$ [49]. The change in the amount of radiation is quantified by means of the parameter $\Delta N_{eff} \equiv N_{eff} - N_{eff}^{SM}$.

Since the fraction of N_1 produced non-thermally becomes non-relativistic at temperatures of the order $\mathcal{O}(eV)$ (see Appendix A), it increases the value of N_{eff} . We remark that the N_1 produced thermally and then diluted does not contribute to ΔN_{eff} because it becomes non-relativistic before equality (see Appendix A).

The contribution to ΔN_{eff} in our model comes therefore from the non-thermal population of N_1 and is mainly controlled by the parameter α :

$$\begin{aligned} \Delta N_{eff} &= \frac{4}{7} \left(\frac{11}{4} \right)^{4/3} \frac{1}{3} (Br(N_2 \rightarrow \mu e N_1) + Br(N_2 \rightarrow \nu_\mu \nu_e N_1)) \left(\frac{g_{s,equality}^4}{g_{s,RH}} \right)^{1/3} \\ &= \frac{4}{7} \left(\frac{11}{4} \right)^{4/3} \frac{1}{3} (1 + \alpha)^{-1} \left(\frac{g_{s,equality}^4}{g_{s,RH}} \right)^{1/3}. \end{aligned} \quad (5.2)$$

According to this, $\alpha = 0$ yields $\Delta N_{eff} \simeq 2.05$ which is excluded by the bounds discussed above. In other words, we need $\alpha > 0$. Future experiments as CMB-S4 will have a sensitivity to constraint $\Delta N_{eff} = 0.060$ (at 95% C.L.) [50]. In the absence of evidence for $\Delta N_{eff} \neq 0$, we will have the limit $\Delta N_{eff} < 0.06$ which requires $\alpha \gtrsim 33$.

5.2 Structure formation (free-streaming)

As dark matter can be classified as cold (CDM), warm (WDM) or hot (HDM) according to its free-streaming λ_{fs} [51], in this section we will roughly estimate the free-streaming of N_1 .

The free-streaming at the epoch of matter-radiation equality is an important parameter that allows us to understand how the first structures were formed. It is given by [52]

$$\lambda_{fs} \equiv \int_{t_{prod}}^{t_e} \frac{\langle v(t) \rangle}{a(t)} dt, \quad (5.3)$$

where t_{prod} is the production time, t_e the equality time, and $\langle v(t) \rangle$ the mean velocity of N_1 .

The N_1 population thermally produced and then diluted due to an injection of entropy is "colder" than what it would be if only thermally produced. The relation between the temperature of the decoupled N_1 and that of the plasma is affected by the injection of entropy, parametrized by Δ , and is given by

$$\frac{T_{N_1}}{T} = \left(\frac{1}{\Delta} \frac{g_s}{g_{s,b}} \right)^{1/3}, \quad (5.4)$$

where the subscript "b" refers to any epoch prior to the dilution.

The thermally produced fraction of a keV N_1 , which is relativistic at production, has its free-streaming suppressed to the scale of $\mathcal{O}(0.1 \text{Mpc})$ due the dilution Δ , being therefore classified as warm or even cold dark matter (see for instance Refs. [43, 51]).

On the other hand, the free-streaming of N_1 produced non-thermally is given by [53, 54]

$$\begin{aligned} \lambda_{fs} &\simeq \int_0^{t_e} \frac{v(t)}{a(t)} dt \\ &\simeq 2v_0 t_e (1+z_e)^2 \ln \left(\frac{1}{v_0 (1+z_e)} + \sqrt{1 + \frac{1}{v_0^2 (1+z_e)^2}} \right), \end{aligned} \quad (5.5)$$

where v_0 is the initial velocity of N_1 and z_e is the red-shift at equality.

Since the non-thermal population of N_1 is produced at T_{RH} through 3-body decay of N_2 , and in the limit of massless final states, we have $p_{prod}^{N_1} \simeq m_{N_2}/3$. For temperatures below T_{RH} , the universe is radiation-dominated and the temperature red-shifts as $a = a_0 \times T_0/T$. We have therefore

$$v_0 \equiv \frac{p_{prod}^{N_1}}{m_{N_1}} a_{prod} \simeq \frac{m_{N_2}}{3m_{N_1}} \frac{T_0}{T_{RH}}. \quad (5.6)$$

For $m_{N_1} = 2.0 \text{ keV}$, $m_{N_2} = 60.0 \text{ GeV}$ and $m_{W'} = 4.7 \times 10^6 \text{ GeV}$ we obtain $\lambda_{fs} \simeq 2.4 \text{ Mpc}$. The non-thermal fraction of N_1 is therefore classified as HDM.

Our non-thermal component can compose up to 50% of the total abundance (for $\alpha = 0$) and 1% (for $\alpha = 10^2$). As the CMB constraint requires $\alpha > 0$, we have a scenario of mixed warm-hot DM. Such a scenario has important implications for structure formation and can address some small-scale problems such as the core-cusp [55]. A rigorous approach to the implications of mixed DM in the structure formation may also put bounds on the parameter α . However this requires the computation of the fluctuation of the power spectrum for our scenario and is beyond the scope of this paper.

6 Conclusions

We investigated the possibility of having a viable mixed warm and hot keV neutrino dark matter in a model based on the $SU(3)_L$ gauge group. Active and sterile neutrinos are arranged in the same $SU(3)_L$ multiplet, with the lightest sterile neutrino being dark matter. Its abundance is set by interactions with Standard Model particles controlled by the new gauge bosons rising from the extended gauge sector. Its stability is warranted by a discrete symmetry that prevents mixing between active and sterile neutrinos, making the model safe from otherwise stringent bounds, such as X-rays.

We have shown that the sterile neutrinos easily thermalize with the Standard Model bath via exchanges of these heavy new gauge bosons, unless their masses are at the GUT scale. When the sterile neutrinos are much lighter than the gauge bosons, they decouple nearly at temperatures much larger than their masses, rendering them ultra-relativistic, and therefore overproduced, at the thermal freeze-out.

In this work, we have shown that this common issue with keV right-handed neutrino is solved within this $SU(3)_L$ gauge group. Since the heavier sterile neutrinos decouple while ultra-relativistic, and are long-lived due to the heavy gauge bosons mediating their decays, they eventually dominate the cosmic expansion after freeze-out. Their out-of-equilibrium decay into SM bath species and also into keV right handed neutrino dark matter. Hence they contribute both to the dilution of warm dark matter population and as well as to its non-thermal HDM population.

Our scenario of mixed warm-hot dark matter is amenable cosmological constraints. As this entropy injection episode should take place before BBN, constraints are derived on the masses of the heavy sterile neutrino states, and gauge bosons. We found that they must be larger than the TeV scale. Moreover, the hot dark matter can also increase N_{eff} in a detectable way, and for this reason we imposed $\alpha \gtrsim 33$ to make sure that the heavy sterile neutrino decay mostly into particles of the $SU(3)_L$ gauge group other than dark matter.

In summary, we conclude that our model can successfully host a mixed warm plus hot dark matter setup in agreement with existing bounds.

Acknowledgments

M.D. acknowledges the support of the Arthur B. McDonald Canadian Astroparticle Physics Research Institute and of the Natural Sciences and Engineering Research Council of Canada. C.A.S.P is supported by the CNPq research grants No. 304423/2017-3. V.O acknowledges CNPq for financial support. FSQ is supported by the São Paulo Research Foundation (FAPESP) through grant 2015/158971, ICTP-SAIFR FAPESP grant 2016/01343-7, CNPq grants 303817/2018-6 and 421952/2018 - 0, and the Serrapilheira Institute (grant number Serra - 1912 - 31613).

A N_1 temperature at the matter-radiation equality

Here we will check when N_1 produced thermally and non-thermally becomes non-relativistic and if they contribute to ΔN_{eff} at CMB.

Following [53, 56], the momentum of N_1 produced non-thermally $p_{N_1}^{NT}$ by N_2 decay gets red-shifted

$$p_{N_1}^{NT}(T) = |p_{N_1}^{NT}(T_D)| \frac{a_D}{a(T)}, \quad (\text{A.1})$$

where a_D is the scale factor at the moment of decay and $p_{N_1}^{NT}(T_D)$ is the momentum of non-thermal N_1 when it is produced. Assuming that $m_{N_2} \gg m_{N_1}, m_{e,\mu,\nu_e,\nu_\mu}$, which imply in

$$|p_{N_1}^{NT}(T_D)| \simeq \frac{m_{N_2}}{3} \quad (\text{A.2})$$

then,

$$p_{N_1}^{NT}(T) = \frac{m_{N_2}}{3} \frac{a_D}{a(T)}. \quad (\text{A.3})$$

We assume that N_1 produced via decay becomes non-relativistic at some temperature T_{nr} (with the respective scale factor a_{nr}). This happen when $p_{N_1}^{NT}(T_{nr}) = m_{N_1}$ [56]. Then, from Eq. (A.3) we have

$$m_{N_1} = \frac{m_{N_2}}{3} \frac{a_D}{a_{nr}}. \quad (\text{A.4})$$

We can represent the red-shift when non-thermal N_1 becomes non-relativistic as

$$Z_{nr}^{NT} + 1 \equiv \frac{a_0}{a_{nr}} = \frac{a_0}{a_D} \frac{a_D}{a_{nr}} \quad (\text{A.5})$$

For a universe dominated by radiation the temperature red-shifting as $T = T_0 \times a_0/a$ and using Eq. (A.4) we obtain

$$Z_{nr}^{NT} + 1 = \frac{3m_{N_1}}{m_{N_2}} \frac{T_D}{T_0} \left(\frac{g_s(T_D)}{g_s(T_0)} \right)^{1/3}, \quad (\text{A.6})$$

where,

$$T_D \simeq T_{RH} = 116 \text{MeV} (1 + \alpha)^{1/2} \left(\frac{70}{g_e(T_{RH})} \right)^{1/4} \left(\frac{m_{N_2}}{100 \text{GeV}} \right)^{5/2} \left(\frac{10^6 \text{GeV}}{M_{W'}} \right)^2. \quad (\text{A.7})$$

As a result of Eq. (A.6) we obtain that N_1 produced non-thermally becomes non-relativistic at temperatures $\mathcal{O}(eV)$ for a long range of α and then contribute to N_{eff} .

On the other hand the red-shift when thermal N_1 becomes non-relativistic is given by:

$$Z_{nr}^T + 1 = \frac{a_0}{a_{nr}} = \frac{a_0}{a_f} \frac{a_f}{a_{nr}}, \quad (\text{A.8})$$

where a_f is the scale factor when N_1 freeze-out at the temperature T_f . The thermal N_1 momentum gets red-shifted

$$p_{N_1}^T(t) = T_f \frac{a_f}{a(t)}. \quad (\text{A.9})$$

However we should note that as the thermal decoupling of N_1 happens before the N_2 decay, the thermal N_1 will be cooler than the bath particles [43], and

$$\frac{a_f}{a} \frac{T_f}{T} = \left(\frac{1}{\Delta} \frac{g_s(T)}{g_s(T_f)} \right)^{1/3}, \quad (\text{A.10})$$

where a and T represent the scale factor and temperature for some epoch after N_2 decays. As non-thermal N_1 is produced during the injection of entropy due decay of N_2 we did not consider this contribution for non-thermal N_1 treatment.

As the thermal N_1 becomes non-relativistic when $p_{N_1}^T \sim m_{N_1}$, therefore from Eq. (A.9) and Eq. (A.10), we can rewrite Eq. (A.8) as

$$Z_{nr}^T + 1 = \frac{m_{N_1}}{T_0} \left(\Delta \frac{g_s(T_f)}{g_s(T_0)} \right)^{1/3}. \quad (\text{A.11})$$

The parameter Δ plays an important role in Z_{nr}^T . For $m_{N_1} = 2.0$ keV and for some α we only have a unique Δ that can reproduce N_1 as DM, such as for $\alpha = 0$ we obtain numerically that we need of $\Delta \simeq 100$ to obtain $\Omega_{N_1} h^2 = 0.12$. As we discussed in Section 4.1 if we increase α we decrease the abundance of non-thermal N_1 which implies that we need to decrease Δ in order to obtain N_1 as DM. Then we can obtain the lower value to Z_{nr}^T for $m_{N_1} = 2.0$ keV if we take a scenario of the minimum allowed Δ value. This scenario can be reproduced if we assume that N_1 is only produced via freeze-out or if we assume that α is so large that non-thermal contribution becomes irrelevant. In these cases we can assume that the lower value to Δ to provide the right amount of relic abundance for N_1 is $\Delta \simeq 19.0$, given by Eq. (3.7) if we take account the dilution factor $Y_{N_1}(T_0) = Y_{N_1}(T_f)/\Delta$

$$\frac{\Omega_{N_1}^0 h^2}{0.12} \simeq \left(\frac{m_{N_1}}{2\text{keV}} \right) \left(\frac{19.0}{\Delta} \right), \quad (\text{A.12})$$

where we take $g_s(T_f) = 100$. For $\Delta = 19.0$ we obtain $Z_{nr}^T = 6.9 \times 10^7 \gg Z_e$, where $Z_e \simeq 3365$ is the red-shift at matter-radiation equality. This is an important result because it shows us that the N_1 produced via freeze-out and consequently diluted by the decay of N_2 becomes non-relativistic before matter-radiation equality epoch.

B Evaluation of ΔN_{eff}

Here we derive Eq. (5.2). At temperature $T \lesssim 0.5$ MeV only the photon (γ), SM neutrinos (ν) and non-thermal N_1 contribute to the radiation energy density of the universe. Then we

can represent the energy density of radiation in that epoch as $\rho_R = \rho_\gamma + N_\nu^{SM} \rho_\nu + \rho_{N_1}$. The energy density for a ultra-relativistic particle (radiation) is given by:

$$\rho_R = \begin{cases} g \frac{7\pi^2}{8} \frac{T^4}{30}, & \text{Fermi-Dirac} \\ g \frac{\pi^2}{30} T^4, & \text{Bose-Einstein} \end{cases} \quad (\text{B.1})$$

where g accounts for its spin degeneracy.

As we discussed in [Section 4](#), we can write the energy density of non-thermal N_1 as function of the energy density of N_2 at the time that N_1 was produced (at T_{RH}), such that $\rho_{N_1} = f_{NT} \cdot \rho_{N_2}(T_{RH})$, with f_{NT} given by [Eq. \(4.8\)](#). According to [\[40, 52\]](#), between the epoch that ρ_{N_2} starts to dominate the energy density of Universe until it decays (at T_{RH}) the radiation produced from decaying of N_2 is the dominant radiation component. Then we can assume that $\rho_{N_2}(T_{RH}) \simeq \rho_R(T_{RH})$. As non-thermal N_1 does not thermalize anymore, its energy density only gets red-shifted. Then we can write the energy density of radiation as

$$\rho_R = \frac{\pi^2}{30} T^4 \left[g_\gamma + \frac{7}{8} g_\nu \left(\frac{T_\nu}{T} \right)^4 \overbrace{\left[N_\nu^{SM} + f_{NT} \cdot \frac{g_e(T_{RH})}{g_\nu} \frac{8}{7} \left(\frac{T}{T_\nu} \right)^4 \left(\frac{T_{N_1}^{RH}}{T} \right)^4 \right]}^{N_{eff}} \right], \quad (\text{B.2})$$

where T_ν represents the temperature of SM neutrinos and $T_{N_1}^{RH}$ is the temperature of N_1 at the time of production (where $T_{N_1}^{RH} = T_{RH}$, after that $T_{N_1}^{RH}$ gets red-shifted). As $g_\nu = 2$, $T/T_\nu = (11/4)^{1/3}$ [\[52\]](#) and using the value of f_{NT} given by [Eq. \(4.8\)](#) we can obtain ΔN_{eff} from [Eq. \(B.2\)](#)

$$\Delta N_{eff} = \frac{1}{3} (1 + \alpha)^{-1} \cdot g_e(T_{RH}) \frac{4}{7} \left(\frac{11}{4} \right)^{4/3} \left(\frac{T_{N_1}^{RH}}{T} \right)^4. \quad (\text{B.3})$$

However we would like to know the ΔN_{eff} at matter-radiation equality epoch T_e . As the temperature of N_1 gets red-shifted after its production, we represent the temperature of N_1 at equality by $T_{N_1}^e = T_{N_1}^{RH} \times a_{RH}/a_e$. From entropy conservation we have $g_s(T_{RH}) T_{RH}^3 a_{RH} = g_s(T_e) T_e^3 a_e^3$, then

$$\frac{1}{T_e^3} \left(\overbrace{\frac{T_{N_1}^e}{T_{N_1}^{RH} a_{RH}}}^{a_e} \right)^3 = \frac{g_s(T_e)}{g_s(T_{RH})}, \quad (\text{B.4})$$

and we obtain

$$\Delta N_{eff} = \frac{4}{7} \left(\frac{11}{4} \right)^{4/3} \frac{1}{3} (1 + \alpha)^{-1} \left(\frac{g_{s,equality}^4}{g_{s,RH}} \right)^{1/3}. \quad (\text{B.5})$$

References

- [1] WMAP collaboration, *Nine-Year Wilkinson Microwave Anisotropy Probe (WMAP) Observations: Cosmological Parameter Results*, *Astrophys. J. Suppl.* **208** (2013) 19 [[1212.5226](#)].
- [2] PLANCK collaboration, *Planck 2018 results. VI. Cosmological parameters*, *Astron. Astrophys.* **641** (2020) A6 [[1807.06209](#)].
- [3] J. R. Primack and M. A. K. Gross, *Hot Dark Matter in Cosmology*. Springer Berlin Heidelberg, Berlin, Heidelberg, 2001, [10.1007/978-3-662-04597-8_12](#), [[astro-ph/0007165](#)].
- [4] G. Bertone, D. Hooper and J. Silk, *Particle dark matter: Evidence, candidates and constraints*, *Phys. Rept.* **405** (2005) 279 [[hep-ph/0404175](#)].
- [5] G. Arcadi, M. Dutra, P. Ghosh, M. Lindner, Y. Mambrini, M. Pierre et al., *The waning of the WIMP? A review of models, searches, and constraints*, *Eur. Phys. J. C* **78** (2018) 203 [[1703.07364](#)].
- [6] P. Bull et al., *Beyond Λ CDM: Problems, solutions, and the road ahead*, *Phys. Dark Univ.* **12** (2016) 56 [[1512.05356](#)].
- [7] R. N. Mohapatra and J. C. Pati, *A Natural Left-Right Symmetry*, *Phys. Rev. D* **11** (1975) 2558.
- [8] G. Senjanovic and R. N. Mohapatra, *Exact Left-Right Symmetry and Spontaneous Violation of Parity*, *Phys. Rev. D* **12** (1975) 1502.
- [9] G. Senjanovic, *Spontaneous Breakdown of Parity in a Class of Gauge Theories*, *Nucl. Phys. B* **153** (1979) 334.
- [10] R. N. Mohapatra and R. E. Marshak, *Local B-L Symmetry of Electroweak Interactions, Majorana Neutrinos and Neutron Oscillations*, *Phys. Rev. Lett.* **44** (1980) 1316.
- [11] T. Appelquist, B. A. Dobrescu and A. R. Hopper, *Nonexotic Neutral Gauge Bosons*, *Phys. Rev. D* **68** (2003) 035012 [[hep-ph/0212073](#)].
- [12] L. Basso, A. Belyaev, S. Moretti and C. H. Shepherd-Themistocleous, *Phenomenology of the minimal B-L extension of the Standard model: Z' and neutrinos*, *Phys. Rev. D* **80** (2009) 055030 [[0812.4313](#)].
- [13] S. Khalil, *TeV-scale gauged B-L symmetry with inverse seesaw mechanism*, *Phys. Rev. D* **82** (2010) 077702 [[1004.0013](#)].
- [14] M. Singer, J. W. F. Valle and J. Schechter, *Canonical Neutral Current Predictions From the Weak Electromagnetic Gauge Group $SU(3) \times u(1)$* , *Phys. Rev. D* **22** (1980) 738.
- [15] J. C. Montero, F. Pisano and V. Pleitez, *Neutral currents and GIM mechanism in $SU(3)$ -L \times $U(1)$ -N models for electroweak interactions*, *Phys. Rev. D* **47** (1993) 2918 [[hep-ph/9212271](#)].
- [16] R. Foot, H. N. Long and T. A. Tran, *$SU(3)_L \otimes U(1)_N$ and $SU(4)_L \otimes U(1)_N$ gauge models with right-handed neutrinos*, *Phys. Rev. D* **50** (1994) R34 [[hep-ph/9402243](#)].
- [17] M. Drewes et al., *A White Paper on keV Sterile Neutrino Dark Matter*, *JCAP* **01** (2017) 025 [[1602.04816](#)].
- [18] E. W. Kolb and M. S. Turner, *The Early Universe*, vol. 69. 1990.
- [19] J. A. Dror, D. Dunsky, L. J. Hall and K. Harigaya, *Sterile Neutrino Dark Matter in Left-Right Theories*, *JHEP* **07** (2020) 168 [[2004.09511](#)].

[20] F. Bezrukov, H. Hettmansperger and M. Lindner, *keV sterile neutrino Dark Matter in gauge extensions of the Standard Model*, *Phys. Rev. D* **81** (2010) 085032 [[0912.4415](#)].

[21] M. Nemevsek, G. Senjanovic and Y. Zhang, *Warm Dark Matter in Low Scale Left-Right Theory*, *JCAP* **07** (2012) 006 [[1205.0844](#)].

[22] A. G. Dias, C. A. de S. Pires and P. S. Rodrigues da Silva, *Naturally light right-handed neutrinos in a 3-3-1 model*, *Phys. Lett. B* **628** (2005) 85 [[hep-ph/0508186](#)].

[23] H. N. Long, *The 331 model with right handed neutrinos*, *Phys. Rev. D* **53** (1996) 437 [[hep-ph/9504274](#)].

[24] C. A. de S. Pires and P. S. Rodrigues da Silva, *Scalar Bilepton Dark Matter*, *JCAP* **12** (2007) 012 [[0710.2104](#)].

[25] J. K. Mizukoshi, C. A. de S. Pires, F. S. Queiroz and P. S. Rodrigues da Silva, *WIMPs in a 3-3-1 model with heavy Sterile neutrinos*, *Phys. Rev. D* **83** (2011) 065024 [[1010.4097](#)].

[26] J. D. Ruiz-Alvarez, C. A. de S. Pires, F. S. Queiroz, D. Restrepo and P. S. Rodrigues da Silva, *On the Connection of Gamma-Rays, Dark Matter and Higgs Searches at LHC*, *Phys. Rev. D* **86** (2012) 075011 [[1206.5779](#)].

[27] S. Profumo and F. S. Queiroz, *Constraining the Z' mass in 331 models using direct dark matter detection*, *Eur. Phys. J. C* **74** (2014) 2960 [[1307.7802](#)].

[28] C. Kelso, C. A. de S. Pires, S. Profumo, F. S. Queiroz and P. S. Rodrigues da Silva, *A 331 WIMP γ Dark Radiation Model*, *Eur. Phys. J. C* **74** (2014) 2797 [[1308.6630](#)].

[29] P. V. Dong, D. T. Huong, F. S. Queiroz and N. T. Thuy, *Phenomenology of the 3-3-1-1 model*, *Phys. Rev. D* **90** (2014) 075021 [[1405.2591](#)].

[30] D. Cogollo, A. X. Gonzalez-Morales, F. S. Queiroz and P. R. Teles, *Excluding the Light Dark Matter Window of a 331 Model Using LHC and Direct Dark Matter Detection Data*, *JCAP* **11** (2014) 002 [[1402.3271](#)].

[31] C. Kelso, H. N. Long, R. Martinez and F. S. Queiroz, *Connection of $g - 2_\mu$, electroweak, dark matter, and collider constraints on 331 models*, *Phys. Rev. D* **90** (2014) 113011 [[1408.6203](#)].

[32] A. Alves, G. Arcadi, P. V. Dong, L. Duarte, F. S. Queiroz and J. W. F. Valle, *Matter-parity as a residual gauge symmetry: Probing a theory of cosmological dark matter*, *Phys. Lett. B* **772** (2017) 825 [[1612.04383](#)].

[33] P. V. Dong, D. T. Huong, F. S. Queiroz, J. W. F. Valle and C. A. Vaquera-Araujo, *The Dark Side of Flipped Trinification*, *JHEP* **04** (2018) 143 [[1710.06951](#)].

[34] J. C. Montero, C. A. De S. Pires and V. Pleitez, *Neutrino masses through the seesaw mechanism in 3-3-1 models*, *Phys. Rev. D* **65** (2002) 095001 [[hep-ph/0112246](#)].

[35] D. Cogollo, H. Diniz and C. A. de S. Pires, *KeV right-handed neutrinos from type II seesaw mechanism in a 3-3-1 model*, *Phys. Lett. B* **677** (2009) 338 [[0903.0370](#)].

[36] P. V. Dong and H. N. Long, *Neutrino masses and lepton flavor violation in the 3-3-1 model with right-handed neutrinos*, *Phys. Rev. D* **77** (2008) 057302 [[0801.4196](#)].

[37] K. Griest and D. Seckel, *Three exceptions in the calculation of relic abundances*, *Phys. Rev. D* **43** (1991) 3191.

[38] T. Hahn, *CUBA: A Library for multidimensional numerical integration*, *Comput. Phys. Commun.* **168** (2005) 78 [[hep-ph/0404043](#)].

[39] U. Seljak, A. Makarov, P. McDonald and H. Trac, *Can sterile neutrinos be the dark matter?*, *Phys. Rev. Lett.* **97** (2006) 191303 [[astro-ph/0602430](#)].

[40] R. J. Scherrer and M. S. Turner, *Decaying particles do not “heat up” the universe*, *Phys. Rev. D* **31** (1985) 681.

[41] C. Cosme, M. Dutra, T. Ma, Y. Wu and L. Yang, *Neutrino Portal to FIMP Dark Matter with an Early Matter Era*, [2003.01723](#).

[42] T. Hasegawa, N. Hiroshima, K. Kohri, R. S. L. Hansen, T. Tram and S. Hannestad, *MeV-scale reheating temperature and thermalization of oscillating neutrinos by radiative and hadronic decays of massive particles*, *JCAP* **12** (2019) 012 [[1908.10189](#)].

[43] A. V. Patwardhan, G. M. Fuller, C. T. Kishimoto and A. Kusenko, *Diluted equilibrium sterile neutrino dark matter*, *Phys. Rev. D* **92** (2015) 103509 [[1507.01977](#)].

[44] G. M. Fuller, C. T. Kishimoto and A. Kusenko, *Heavy sterile neutrinos, entropy and relativistic energy production, and the relic neutrino background*, [1110.6479](#).

[45] Q.-H. Cao and D.-M. Zhang, *Collider Phenomenology of the 3-3-1 Model*, [1611.09337](#).

[46] Y. A. Coutinho, V. Salustino Guimarães and A. A. Nepomuceno, *Bounds on Z' from 3-3-1 model at the LHC energies*, *Phys. Rev. D* **87** (2013) 115014 [[1304.7907](#)].

[47] D. Cogollo, F. F. Freitas, C. A. de S. Pires, Y. M. Oviedo-Torres and P. Vasconcelos, *Deep learning analysis of the inverse seesaw in a 3-3-1 model at the LHC*, *Phys. Lett. B* **811** (2020) 135931 [[2008.03409](#)].

[48] T. B. de Melo, S. Kovalenko, F. S. Queiroz, C. Siqueira and Y. S. Villamizar, *Rare Kaon Decay to Missing Energy: Implications of the NA62 Result for a Z' Model*, [2102.06262](#).

[49] G. Mangano, G. Miele, S. Pastor, T. Pinto, O. Pisanti and P. D. Serpico, *Relic neutrino decoupling including flavor oscillations*, *Nucl. Phys. B* **729** (2005) 221 [[hep-ph/0506164](#)].

[50] K. Abazajian et al., *CMB-S4 Science Case, Reference Design, and Project Plan*, [1907.04473](#).

[51] A. Merle, V. Niro and D. Schmidt, *New Production Mechanism for keV Sterile Neutrino Dark Matter by Decays of Frozen-In Scalars*, *JCAP* **03** (2014) 028 [[1306.3996](#)].

[52] E. W. Kolb and M. S. Turner, *The Early Universe*, vol. 69. Westview Press.

[53] S. Borgani, A. Masiero and M. Yamaguchi, *Light gravitinos as mixed dark matter*, *Phys. Lett. B* **386** (1996) 189 [[hep-ph/9605222](#)].

[54] W. B. Lin, D. H. Huang, X. Zhang and R. H. Brandenberger, *Nonthermal production of WIMPs and the subgalactic structure of the universe*, *Phys. Rev. Lett.* **86** (2001) 954 [[astro-ph/0009003](#)].

[55] M. R. Lovell, V. Eke, C. S. Frenk, L. Gao, A. Jenkins, T. Theuns et al., *The haloes of bright satellite galaxies in a warm dark matter universe*, *Monthly Notices of the Royal Astronomical Society* **420** (2012) 2318 [<https://academic.oup.com/mnras/article-pdf/420/3/2318/3020178/mnras0420-2318.pdf>].

[56] J. Hasenkamp and J. Kersten, *Dark radiation from particle decay: cosmological constraints and opportunities*, *JCAP* **08** (2013) 024 [[1212.4160](https://arxiv.org/abs/1212.4160)].